

Origin of the exceptional negative thermal expansion in metal-organic framework-5 $\text{Zn}_4\text{O}(\text{1,4-benzenedicarboxylate})_3$

W. Zhou* and H. Wu

*NIST Center for Neutron Research, National Institute of Standards and Technology, Gaithersburg, Maryland 20899, USA
and Department of Materials Science and Engineering, University of Maryland, College Park, Maryland 20742, USA*

T. Yildirim†

*NIST Center for Neutron Research, National Institute of Standards and Technology, Gaithersburg, Maryland 20899, USA
and Department of Materials Science and Engineering, University of Pennsylvania, Philadelphia, Pennsylvania 19104, USA*

J. R. Simpson and A. R. Hight Walker

Optical Technology Division, Physics Laboratory, National Institute of Standards and Technology, Gaithersburg, Maryland 20899, USA

(Received 30 May 2008; published 20 August 2008)

Metal organic framework-5 (MOF-5) was recently suggested to possess an exceptionally large negative thermal-expansion coefficient. Our direct experimental measurement of the thermal expansion of MOF-5 using neutron powder diffraction, in the temperature range of 4 to 600 K, shows that the linear thermal-expansion coefficient is $\approx -16 \times 10^{-6} \text{ K}^{-1}$. To understand the origin of this large negative thermal-expansion behavior, we performed first-principles lattice dynamics calculations. The calculated thermal-expansion coefficients within quasiharmonic approximation agree well with the experimental data. We found that almost all low-frequency lattice vibrational modes (below $\sim 23 \text{ meV}$) involve the motion of the benzene rings and the ZnO_4 clusters as rigid units and the carboxyl groups as bridges. These so-called “rigid-unit modes” exhibit various degrees of phonon softening (i.e., the vibrational energy decreases with contracting crystal lattice) and thus are directly responsible for the large negative thermal expansion in MOF-5. Initial efforts were made to observe the phonon softening experimentally.

DOI: [10.1103/PhysRevB.78.054114](https://doi.org/10.1103/PhysRevB.78.054114)

PACS number(s): 65.40.De, 63.20.-e, 61.05.F-

I. INTRODUCTION

Negative thermal expansion (NTE) of materials (i.e., materials contract upon heating) over an extended temperature range is an unusual material property with a variety of potential technological applications. Only a few families of materials are known to exhibit considerable NTE behavior such as the AM_2O_8 ($A=\text{Zr, Hf}; M=\text{V}$) family, the AM_2O_7 ($A=\text{U, Th, Zr, Hf, Sn}; M=\text{P, V}$) family, the cuprite structures (e.g., Cu_2O and Ag_2O), some tetrahedrally coordinated structures (e.g., CuCl), and some zeolites/zeolitelike materials.¹⁻⁴ Recently, a family of cyanide-based coordination framework materials was also found to possess NTE coefficients.^{5,6}

Metal organic frameworks (MOFs), consisting of metal atoms or clusters and organic linkers, are a relatively new class of nanoporous crystalline materials. Due to their unique nanoporous framework structures, many novel properties and potential applications have been identified.⁷⁻¹¹ In addition, they also exhibit certain properties similar to those found in their inorganic counterparts, zeolitelike materials, and non-porous metal organic coordination framework materials. Indeed, it was recently suggested that MOF-5 [chemical formula: $\text{Zn}_4\text{O}_{13}(\text{C}_8\text{H}_4\text{O}_4)_3$, see Fig. 1], the most well-known MOF compound, also exhibits an exceptional negative thermal-expansion behavior¹²⁻¹⁴ as found in some zeolites/zeolitelike materials.

Experimentally, there exists some indirect evidence supporting the NTE of MOF-5. In particular, it was observed that MOF-5 with adsorbed N_2 or CO_2 expands upon cooling.^{12,13} Yet, no direct thermal-expansion measurement

on a clean MOF-5 sample has been reported so far. Theoretically, a recent molecular-dynamics (MD) simulation¹³ predicted that MOF-5 has a very large linear thermal-expansion coefficient [$\alpha=(1/a)(da/dT)$] of $\approx -20 \times 10^{-6} \text{ K}^{-1}$. Another MD study¹⁴ suggested a linear thermal-expansion coefficient of $\approx -8 \times 10^{-6} \text{ K}^{-1}$ for MOF-5. Both simulations, carried out using classical force field, have provided some insight on the mechanism of the NTE. Nevertheless, MD simulations are essentially “experiments” performed in computers and they do not directly reveal the fundamental physics behind the computational observations. Snapshots of the structure equilibrated at high temperature often contain mixed lattice phonon characteristics, although they provide hints on what kind of motions may be related to the NTE behavior.

Clearly, further investigation (both experimentally and theoretically) is needed to better understand the origin of the large negative thermal expansion in MOF-5. The knowledge

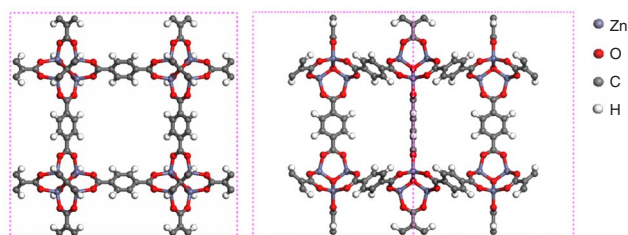


FIG. 1. (Color online) [100] (left) and [110] (right) views of the crystal structure of MOF-5, which consists of BDC linkers connecting ZnO_4 clusters located at the tetrahedral site of an fcc lattice.

obtained would also have practical implications for the general structural stability of MOFs, since most MOF structures start to break apart at an elevated temperature of about 650 K.¹⁵

Here we first directly determined the thermal-expansion coefficient of MOF-5 by variable-temperature neutron-diffraction measurements. Then we performed first-principles lattice-dynamical calculations to investigate the origin of the large negative thermal expansion. Critically, we found that most of the low-frequency lattice phonon modes exhibit phonon softening behaviors (i.e., the vibrational energy decreases with contracting crystal lattice), which are fully responsible for the large negative thermal expansion. Finally, we describe our efforts to observe the phonon softening experimentally via variable-temperature Raman and inelastic neutron scatterings.

II. MATERIALS AND METHODS

The MOF-5 sample used in the experiment is the same as what we used in our previous H₂ adsorption studies.^{16,17} The diffraction measurement was performed with the BT-1 high-resolution powder diffractometer at the NIST Center for Neutron Research (NCNR). A deuterated MOF-5 sample was used to avoid the large incoherent scattering of the H element. Using a triple grating spectrometer, Raman spectra were measured in the low-frequency range (down to ~ 20 cm⁻¹) on the normally hydrogenated sample. Several laser excitations at wavelengths ranging from 465.8 to 773.3 nm were used. Densities of states of low-energy phonons were probed on the disk-chopper spectrometer (DCS) at NCNR, also using a normal hydrogenated sample.

First-principles calculations were performed within the plane-wave implementation of density-functional theory (DFT) in the PWSCF package.¹⁸ We used Vanderbilt-type ultrasoft potential. Lattice dynamics calculations were performed using the small-displacement method, the same scheme as what we used in our previous work,¹⁹ except that a larger cut-off energy of 680 eV was used in the current work in order to obtain more accurate phonon frequencies needed in the thermal-expansion calculation. In addition, we tested both the local-density approximation (LDA) and the generalized gradient approximation (GGA).

III. RESULTS AND DISCUSSION

MOF-5 consists of Zn₄O clusters linked by 1,4-benzenedicarboxylate (BDC) possessing a fcc crystal structure^{7,16} as schematically shown in Fig. 1. Using neutron powder diffraction, we directly measured the linear lattice thermal-expansion coefficient of MOF-5 in the temperature range of 4 to 600 K (note that MOF-5 starts to decompose at ~ 650 K). The measured lattice constants and derived linear thermal-expansion coefficients are shown as a function of temperature in Figs. 2(a) and 2(b), respectively. The experimental thermal-expansion coefficient was found to be $\approx -16 \times 10^{-6}$ to -10×10^{-6} K⁻¹ in the temperature range investigated. Apparently, previous MD studies^{13,14} correctly

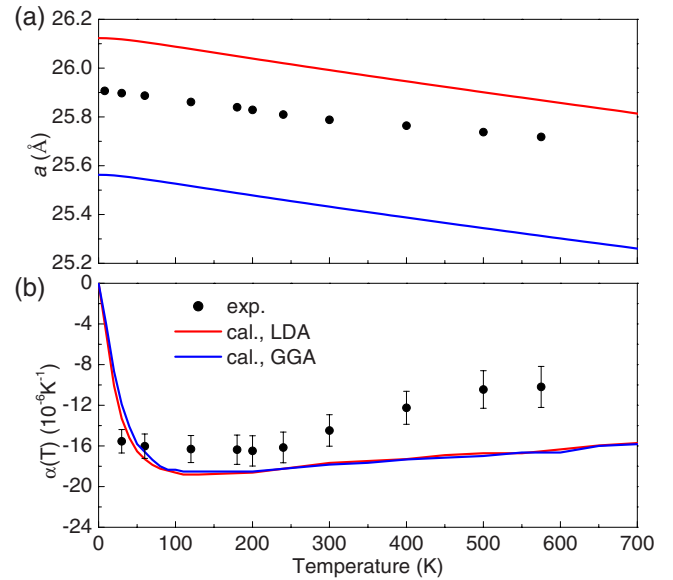


FIG. 2. (Color online) (a) The experimental (dots) and calculated (lines) temperature dependence of the lattice constant a of MOF-5. (b) The experimental (dots) and calculated (lines) linear thermal-expansion coefficient of MOF-5. Note that the experimental data points of a have very small error bar ($<0.01\%$) while the errors associated with the derived data points of α are large ($\sim 10\%$). This is due to the limited number of a data points used in the numerical interpolation and differentiation. Computationally, LDA underestimates the lattice constant while GGA gives overestimated result as generally expected. Nevertheless, both LDA and GGA generate nearly the same linear thermal-expansion coefficients, which agree reasonably well with the experimental data.

predicted the sign of the thermal expansion and its order of magnitude.

Next, we discuss the origin of the large negative thermal expansion. There are four general mechanisms resulting in NTE: (i) shortening of bond lengths and phase changes; (ii) bridging atoms and rigid-unit vibrational modes (RUMs); (iii) magnetostriction; and (iv) electronic effects.¹ The “bridging atoms and RUM” mechanism is responsible for the NTE in many coordination framework materials¹ (e.g., ZrW₂O₈, ZrV₂O₇, AlPO₄-17, Zn(CN)₂, various zeolite frameworks, etc.), and thus is very likely applicable to MOF-5. As speculated in the previous MD study, the main contribution to the large NTE could originate from the coordination bonds of the oxygen atoms of the carboxylate groups to the zinc atoms of the corners.¹² In the language of the RUM, the ZnO₄ tetrahedra and the benzene rings in the BDC linkers can be regarded as structural anchors because of their relatively strong rigidity. The O atoms shared by four ZnO₄ tetrahedra and the flexible carboxylate groups serve as bridges between the rigid units. This is schematically shown in Fig. 3. Following the RUM argument, the large amplitude transverse vibration of the bridge (particularly, the carboxylate groups) leads to the reduction in the average bridge length, which would then result in NTE.

The RUM mechanism certainly provides a general topological picture to understand the NTE in framework materials. More detailed lattice dynamics analysis is, however, es-

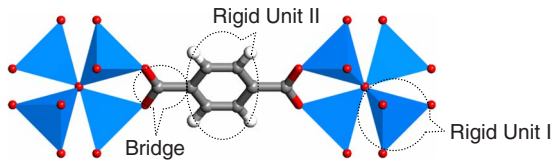


FIG. 3. (Color online) According to the “rigid-unit modes” mechanism, the ZnO₄ tetrahedra and the benzene rings serve as the rigid units while the carboxyl groups serve as the bridge. The large amplitude transverse vibration of the bridge leads to negative thermal expansion.

essential to understand the NTE quantitatively and at the atomic level. It is particularly important to find out exactly what types of RUMs does the MOF-5 crystal support.

We have previously investigated the lattice dynamics of MOF-5 at its equilibrium low-temperature structure.¹⁹ Most relevant to the negative thermal expansion are those low-frequency phonon modes, which involve the motion of the ZnO₄ clusters and the benzene rings as rigid units. How these modes contribute to the negative thermal expansion requires phonon calculations at various temperatures. On the other hand, thermal expansion in insulators is known to arise from anharmonic lattice vibrations; thus, thermal expansion can be calculated within quasiharmonic approximation. Here, we obtain the temperature dependence of the MOF-5 lattice parameters a by minimizing the Helmholtz free energy,

$$F(a, T) = V(a) + \sum_j \sum_{\mathbf{q}} \left\{ \frac{1}{2} \hbar \omega_j(\mathbf{q}) + kT \ln(1 - e^{-\hbar \omega_j(\mathbf{q})/kT}) \right\}, \quad (1)$$

where the first term is the ground-state energy and the second term is obtained by summing the phonon modes over the wave vectors in the Brillouin zone. In the quasiharmonic approximation, the effect of the anharmonicity in the lattice energy is treated by allowing the phonon frequencies to depend on the lattice parameters. Hence, for a given temperature T , we first take a , minimize the atomic positions, and calculate the phonon spectrum (a detailed description of our phonon calculations can be found in Ref. 19) and then the free energy. Repeating this for other values of a , we find the optimum value of the lattice parameter that minimizes the free energy at a given temperature. In this way, one obtains the temperature dependence of a . The results are shown as solid lines in Fig. 2(a). The derived thermal-expansion coefficients are shown in Fig. 2(b). Compared to the experimental result, LDA underestimates the lattice constant while GGA gives an overestimated value as generally expected. Nevertheless, the two generate nearly the same linear thermal-expansion coefficients, which are also in reasonably good agreement with the experimental data. Note that as an intrinsic limitation of the quasiharmonic approximation, the anharmonic contribution and thus the calculated thermal expansion at 0 K are always zero. In contrast, the anharmonic effect in the real material can be large at very low temperature. This may be responsible for the small difference be-

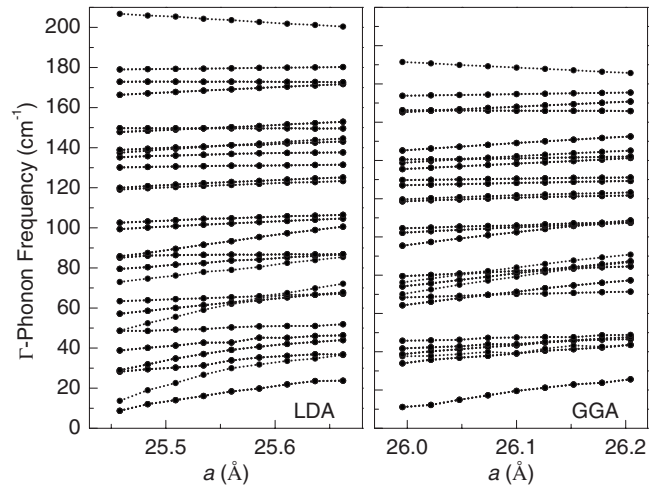


FIG. 4. Calculated phonon frequency at Γ as a function of lattice constant a . Only the low-energy portion is shown. Note that nearly all optical-phonon modes below 180 cm⁻¹ exhibit phonon softening to various extent. In contrast, phonon modes with higher frequencies (not shown here) exhibit normal behavior, i.e., the phonon frequencies increase with contracting lattice. Note that 1 meV \cong 8.07 cm⁻¹.

tween the experimental results and our calculations at temperature close to zero.

From Eq. (1), it is clear that how the energies of the phonon modes change with lattice constants plays a critical role in determining the thermal expansion. If phonons soften on contraction of the lattice (i.e., the Grüneisen parameters are negative), it could lead to thermal contraction. Interestingly, we found that this is exactly what happens for the majority of the 67 optical-phonon modes below \sim 23 meV, which involve the motion of the ZnO₄ cluster and the benzene ring as a whole. All these modes to a certain extent can be regarded as the RUMs in the topological model discussed earlier. In Fig. 4, we show explicitly the calculated phonon frequency at the zone center as a function of lattice constant a for these low-energy modes. Phonon modes with higher frequencies show normal behavior, i.e., the phonon frequencies increase with the contracting lattice and thus are not shown. It is unusual that there exists such a large group of soft phonons, which contribute to the exceptional negative thermal expansion of MOF-5.

To obtain a more direct and intuitive understanding on how the soft-phonon modes result in NTE and how they relate to the general RUM mechanism, we now inspect the low-frequency modes individually. In Fig. 5, we show images of selected representative phonon modes. The lowest energy phonon mode involves the translational motion of the BDC linker along the direction perpendicular to the benzene plane [Fig. 5(a)]. The second lowest energy modes involve the whole organic linkers twisting around the crystal axis direction [Fig. 5(b)]. All other modes with $E < 23$ meV are also various combinations of the motion of the C₆H₄ rings and the vibration of the ZnO₄ clusters as rigid units [e.g., Figs. 5(c)–5(h)]. In other words, all these modes can be viewed as results of local deformations (translation, rotation,

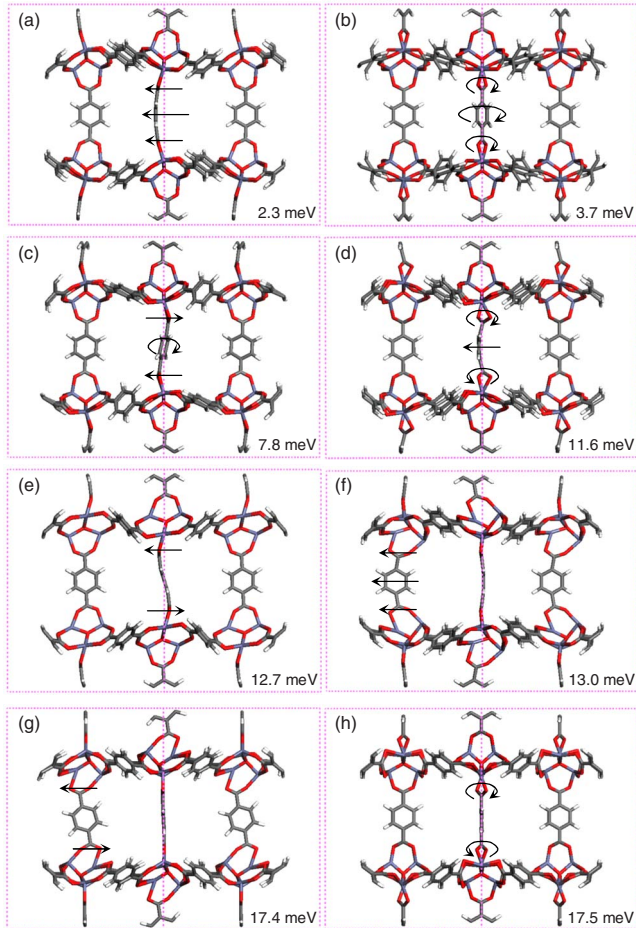


FIG. 5. (Color online) Schematics of several representative low-frequency phonon modes. Corresponding phonon energies from LDA calculation at 0 K are also shown. Note that all the phonon modes below 23 meV originate from various combinations of local motions of the bridging carboxyl groups.

and twisting) of the bridging carboxyl groups. In accord with the RUM mechanism, the population of these vibrational modes clearly has the effect of pulling the anchoring ZnO_4 clusters closer, which results in reduced lattice constant at high temperature.

So far, we have demonstrated theoretically that a large group of low-frequency phonons is responsible for the large negative thermal expansion in MOF-5. It would be valuable to experimentally observe the phonon softening phenomenon. Since the lattice constant is a function of both pressure and temperature, the phonon softening can be accessed by changing either of them. However, the MOF-5 structure is highly porous. It is not trivial to find an appropriate pressure-transmitting medium, which would not penetrate the crystal structure. Therefore, our initial experimental effort was focused on changing the sample temperature. We predicted a number of Raman-active phonon modes¹⁹ and thus measured temperature-dependent Raman spectra of MOF-5 in an optical cryostat (4 to 400 K) under vacuum (zero external pressure). Unfortunately, the intensity of most of the Raman-active modes proves too weak for measurement. We

observed only one Raman peak at $\sim 42 \text{ cm}^{-1}$ in the low-frequency range of interest (0 to 200 cm^{-1}). This peak did not shift noticeably in frequency (to within our measurement certainty) between 4.5 K and room temperature. A strong fluorescence background (quantum dot effect) from the ZnO_4 clusters²⁰ complicates the determination of a Raman peak shift with temperature and the observation of any additional modes. Then we turned to the inelastic neutron scattering technique. Unlike Raman scattering, which applies selection rules, inelastic neutron scattering probes all phonon modes. Unfortunately, the measured spectra have large background at elevated temperature due to the broadening of the phonon peaks and multiphonon scattering and thus are not conclusive. Further experimental study is clearly needed to unambiguously identify those soft phonons. Ideally, a pressure- or temperature-dependent measurement of the phonon dispersion on a single-crystal sample would provide the ultimate experimental evidence for the phonon softening.

Finally, we note that the phonon softening also has important implications for the structural stability of MOF-5. As implied in Fig. 4, the lowest energy phonon modes can easily turn “negative” in frequency with a large enough lattice contraction at high temperature and thus introduce structural instability (i.e., lowered crystal symmetry and then breakage between the zinc oxide cluster and the organic linker). Indeed, under ambient pressure, the MOF-5 sample starts to decompose at $\sim 650 \text{ K}$ and eventually turns into ZnO powders. Clearly, the chemical bonds bridging the benzene rings and the ZnO_4 units are the most unstable part of the MOF-5 structure. This is further supported by the fact that the organic linker molecules in the precursor acids usually have higher thermal stability than their counterparts in the corresponding MOF structures. For example, the benzene-1,4-dicarboxylic acid (organic precursor of MOF-5) melts or sublimates at $\sim 700 \text{ K}$ and decomposes (i.e., breaks covalent bonds) at a much higher temperature ($>1000 \text{ K}$).

IV. CONCLUSIONS

In summary, we have measured the thermal expansion of MOF-5 experimentally and the linear thermal-expansion coefficient was found to be $\approx -16 \times 10^{-6} \text{ K}^{-1}$. Our calculated thermal expansion based on DFT reproduced the experimental data reasonably well. The phonon softening of the low-frequency lattice modes is responsible for the large negative thermal expansion in MOF-5. Most lattice phonon modes below $\sim 23 \text{ meV}$ can be regarded as rigid-unit modes. Note that not all MOF materials show NTE behavior. The carboxyl group, which is “flexible” enough, plays a key role in enabling MOF-5 to support those RUMs. Other MOFs with a similar structural motif [e.g., isoreticular metal organic framework (IRMOF)-2 through -16] (Ref. 8) are all expected to have similar dramatic NTE as MOF-5. MOFs with different symmetries and configurations, which do not possess flexible structural units or chemical bonds that can serve as bridges between rigid units, would not be expected to show much negative thermal-expansion behavior. For example, zeolitic imidazolate framework-8 ($\text{Zn}_6\text{N}_{24}\text{C}_{48}\text{H}_{60}$, space group $I4-3m$) consists of rigid units of ZnN_4 and a methyl-

-imidazolate ring.²¹ The two rigid units are directly connected through the N atom without an additional buffering bridge. Not surprisingly, we found the experimental linear thermal-expansion coefficient of zeolitic imidazolate framework-8 to be positive ($\approx 10 \times 10^{-6} \text{ K}^{-1}$).

ACKNOWLEDGMENTS

The authors thank C. M. Brown and Y. Qiu for their technical help in the DCS data collection. We acknowledge partial support from DOE BES with Grant No. DE-FG02-98ER45701.

*wzhou@nist.gov

†taner@nist.gov

¹G. D. Barrera, J. A. O. Bruno, T. H. K. Barron, and N. L. Allan, *J. Phys.: Condens. Matter* **17**, R217 (2005).

²S. a Beccara, G. Dalba, P. Fornasini, R. Grisenti, A. Sanson, and F. Rocca, *Phys. Rev. Lett.* **89**, 025503 (2002).

³A. Sanson, F. Rocca, G. Dalba, P. Fornasini, R. Grisenti, M. Dapiaggi, and G. Artioli, *Phys. Rev. B* **73**, 214305 (2006).

⁴M. Vaccari, R. Grisenti, P. Fornasini, F. Rocca, and A. Sanson, *Phys. Rev. B* **75**, 184307 (2007).

⁵A. L. Goodwin and C. J. Kepert, *Phys. Rev. B* **71**, 140301(R) (2005).

⁶K. W. Chapman, P. J. Chupas, and C. J. Kepert, *J. Am. Chem. Soc.* **128**, 7009 (2006).

⁷H. Li, M. Eddaoudi, M. O’Keeffe, and O. M. Yaghi, *Nature (London)* **402**, 276 (1999).

⁸M. Eddaoudi, J. Kim, N. Rosi, D. Vodak, J. Wachter, M. O’Keeffe, and O. M. Yaghi, *Science* **295**, 469 (2002).

⁹M. Yaghi, M. O’Keeffe, N. W. Ockwig, H. K. Chae, M. Eddaoudi, and J. Kim, *Nature (London)* **423**, 705 (2003).

¹⁰H. K. Chae, D. Y. Siberio-Perez, J. Kim, Y. B. Go, M. Eddaoudi, A. J. Matzger, M. O’Keeffe, and O. M. Yaghi, *Nature (London)* **427**, 523 (2004).

¹¹N. Ockwig, O. D. Friedrichs, M. O’Keeffe, and O. M. Yaghi,

Acc. Chem. Res. **38**, 176 (2005).

¹²J. L. C. Rowsell, E. C. Spencer, J. Eckert, J. A. K. Howard, and O. M. Yaghi, *Science* **309**, 1350 (2005).

¹³D. Dubbeldam, K. S. Walton, D. E. Ellis, and R. Q. Snurr, *Angew. Chem., Int. Ed.* **46**, 4496 (2007).

¹⁴S. S. Han and W. A. Goddard III, *J. Phys. Chem. C* **111**, 15185 (2007).

¹⁵J. Hafizovic, M. Bjorgen, U. Olsbye, P. D. C. Dietzel, S. Bordiga, C. Prestipino, C. Lamberti, and K. P. Lillerud, *J. Am. Chem. Soc.* **129**, 3612 (2007).

¹⁶T. Yildirim and M. R. Hartman, *Phys. Rev. Lett.* **95**, 215504 (2005).

¹⁷W. Zhou, H. Wu, M. R. Hartman, and T. Yildirim, *J. Phys. Chem. C* **111**, 16131 (2007).

¹⁸S. Baroni, A. Dal Corso, S. de Gironcoli, P. Giannozzi, C. Cavazzoni, G. Ballabio, S. Scandolo, G. Chiarotti, P. Focher, A. Pasquarello, K. Laasonen, A. Trave, R. Car, N. Marzari, and A. Kokalj (<http://www.pwscf.org/>).

¹⁹W. Zhou and T. Yildirim, *Phys. Rev. B* **74**, 180301(R) (2006).

²⁰S. Bordiga, C. Lamberti, G. Ricchiardi, L. Regli, F. Bonino, A. Damin, K. P. Lillerud, M. Bjorgen, and A. Zecchina, *Chem. Commun. (Cambridge)* **2004**, 2300.

²¹H. Wu, W. Zhou, and T. Yildirim, *J. Am. Chem. Soc.* **129**, 5314 (2007).